Physica A 387 (2008) 4531–4540

Contents lists available at ScienceDirect

Physica A

journal homepage: www.elsevier.com/locate/physa

Tracer diffusion in glassforming liquids

A. Andraca [a], P. Goldstein [a], L.F. del Castillo [b,*]

[a] Departamento de Física, Facultad de Ciencias, Universidad Nacional Autónoma de México, 04510 México D.F., Mexico

[b] Departamento de Polímeros, Instituto de Investigaciones en Materiales, Universidad Nacional Autónoma de México, 04510 México D.F., Mexico

ARTICLE INFO

Article history:
Received 15 May 2007
Received in revised form 28 March 2008
Available online 8 April 2008

Keywords:
Tracer diffusion
Stokes–Einstein relation
Glass forming liquids
Time–temperature superposition principle

ABSTRACT

In the last decades, a wide collection of experimental evidence has been found in the study of supercooled glassformers on the existence of a crossover between two dynamical regimes at a temperature T_c. We discuss the validity of the Vogel–Fulcher–Tammann in both regions. The breakdown of the Stokes–Einstein relation below T_c is presented, indicating that the diffusion coefficient of a tracer becomes decoupled from the viscosity through an exponent ξ, and the diffusion process is intensified. We verify that a temperature shift on the diffusion coefficient introduces the same effect as the Stokes–Einstein breakdown equation. We present the dependence of this exponent on the ratio between the radii of the tracer and the host liquid molecule.

1. Introduction

Relaxation processes that take place in supercooled liquids in the vicinity of the glass transition temperature T_g, have been extensively studied in the last two decades. One of the most significant features of a liquid approaching the glass transition is the rapid increase of the viscosity. Theoretically, many efforts have been undertaken to study the temperature dependence of the viscosity and other thermodynamic properties.

One of the most important empirical equations that deals with the behavior of the viscosity as the system approaches T_g is the Vogel–Fulcher–Tammann (VFT) equation, namely [1–3],

$$\log \eta = A - \frac{B}{T - T_0}, \tag{1}$$

where A and B are independent parameters and T_0 may be interpreted as the isoentropic temperature, namely, the temperature where the configurational entropy vanishes. The relaxation phenomena described by the VFT equation correspond to the very slow α-relaxation processes. One may find, however, that fast relaxation processes occur in the vicinity of T_g, namely the β-relaxation processes [4–14]. Relaxation and diffusion mechanisms present drastic changes around a cross-over temperature T_c which lies within the interval $[1.15T_g, 1.28T_g]$ [15–34]. There are two important aspects that characterize this cross-over region. The VFT equation does no longer describe the experimental results for the viscosity below T_c, and, furthermore, the diffusion mechanisms undergo changes.

The Stokes–Einstein (SE) equation establishes that the diffusion coefficient of a sphere of radius a in a fluid whose viscosity is η, is given by

$$D = \frac{k_B T}{6\pi a \eta}, \tag{2}$$

* Corresponding author. Tel.: +52 55 5622 4723; fax: +52 55 5616 1201.
E-mail address: lfelipe@servidor.unam.mx (L.F. del Castillo).

0378-4371/$ – see front matter © 2008 Elsevier B.V. All rights reserved.
doi:10.1016/j.physa.2008.04.001

where k_B is Boltzmann's constant. In the case of a glassformer at temperatures above T_c, the SE equation works. However, for temperatures below T_c, the SE equation breaks down, and the diffusion process is enhanced. In this region, the influence of the viscous relaxation upon the diffusion coefficient may be expressed in terms of the relation

$$D \propto \eta^{-\xi}, \tag{3}$$

where

$$0 < \xi < 1.$$

In fact, both experimental [35–47] and theoretical [48–56] results have indicated that as a supercooled glass forming liquid is cooled towards T_g, its dynamics becomes increasingly heterogeneous presenting magnified diffusion mechanisms. For temperatures below T_c, one may assume a dynamic heterogeneity consisting of two different mobile domains, more mobile domains that govern the translational molecular displacement and less mobile domains that determine structural relaxation [35]. In this case, the diffusion decouples from the viscosity ($\xi < 1$) due to the so-called microviscosity effect [48] that considers that the viscosity around a small tracer is rather different from that of the bulk due to size effects. The single particle dynamics of the tracer and the collective dynamics of the supercooled liquid, as it is taken towards lower temperatures, occur on different time and length scales. and ξ increases with increasing size of the tracer.

In this work, we present the enhancement of the diffusion coefficient of small tracers in glass formers in the region below the crossover temperature T_c taking into consideration that the VFT equation is not valid for this region, In Section 2 we give a brief presentation of an empirical equation for the viscosity in the temperature range between T_g and T_c. In Section 3, we present the behavior of different tracers in supercooled liquids and we obtain the SE equation breakdown below T_c. We discuss the effect of a temperature shift on the diffusion coefficient by means of the time-temperature superposition principle [35]. In addition, we find different values for the exponent ξ in terms of the ratio between the radius of the tracer and that of the host and the dependence of the exponent with the glass transition temperature of the host. Finally, we present in Section 4 some conclusions,

2. The viscosity

One strong evidence of the crossover of the regimes is that a single VFT equation cannot fit the data for the viscosity in the whole range of temperatures from T_g, the glass transition temperature, to T_m, the fusion temperature [5–7,13,21,26–30,57–60]. As we have already discussed these two regimes are separated by the temperature T_c. It has been proven that the experimental data for the viscosity for temperatures above T_c may always be fitted by a VFT equation. In the literature one may find different proposals to fit the data for the viscosity for temperatures below T_c. Some authors propose that a different VFT, namely one with different parameters of those of the VFT fit above T_c, may fit the data below T_c [5,13,26–30,60]. Another empirical equation that is also used to fit the viscosity data is the well known Williams–Landel–Ferry (WLF) equation [61] which actually also fits nicely the data for the viscosity above T_c. One may find proposals where a different WLF equation may also fit the data below T_c [6,7]. There is also strong evidence that the data below T_c must be fitted using different equations, as for example those given in references [13,26,27,56–59]. Stickel's derivative analysis [26,27] provides an excellent way to prove which is the right answer to this question. This method consists of the study of a given equation used to fit the data below T_c in terms of the temperature derivative analysis for the quantities,

$$x = \left\{ f/Hz, \sigma_{dc}\varepsilon_0/s^{-1}, \eta^{-1}/poise^{-1} \right\}, \tag{4}$$

where f is the frequency of the peak of the loss function, the imaginary part of the complex dielectric function, σ_{dc} is the dc conductivity, and η the viscosity. The method consists on the evaluation of three derivatives of a given empirical form for $\log x$,

$$\left[\frac{\mathrm{d}\log x}{\mathrm{d}T}\right]^{-1/2} \tag{5}$$

$$\frac{\mathrm{d}}{\mathrm{d}T}\left[\left(\frac{\mathrm{d}\log x}{\mathrm{d}T}\right)^{-1/2}\right] \tag{6}$$

$$\Theta = \frac{\frac{\mathrm{d}\log x}{\mathrm{d}T}}{\frac{\mathrm{d}^2\log x}{\mathrm{d}T^2}} \tag{7}$$

and the comparison of the values of the derivatives for the given form and the VFT equation, finding whether experimental data fit VFT or not.

In this work, we propose an empirical form for the viscosity for the $T < T_c$ region which has already been discussed in a previous work [56], namely,

$$\log \frac{\eta(T^*)}{\eta(T)} = C\,(T_A - T)^2 + E \tag{8}$$

Table 1
Values for the coefficients and temperature T_A given in Eq. (8) for the glasssformers here considered and the values of the χ^2 test and of the correlation coefficient R^2

Glassformer	C	E	T_A(K)	χ^2	R^2
Salol	−0.0025	9.686	282	0.00058	0.99993
PDE	−0.0019	9.063	362	0.00695	0.99791
OTP	−0.0024	11.956	310	0.00417	0.99569
TNB	−0.0008	10.740	453	0.00049	0.99993

Table 2
Values for the parameters of the VFT equation, Eq. (9) for the glasssformers here considered and the values of the χ^2 test and of the correlation coefficient R^2

Glassformer	A	B	T_0(K)	χ^2	R^2
Salol	10.733	483	175	0.0036	0.9931
PDE	12.161	324	278	7.25×10^{-8}	1
OTP	17.763	675	202	0.0050	0.9931
TNB	14.700	433	330	0.0031	0.9956

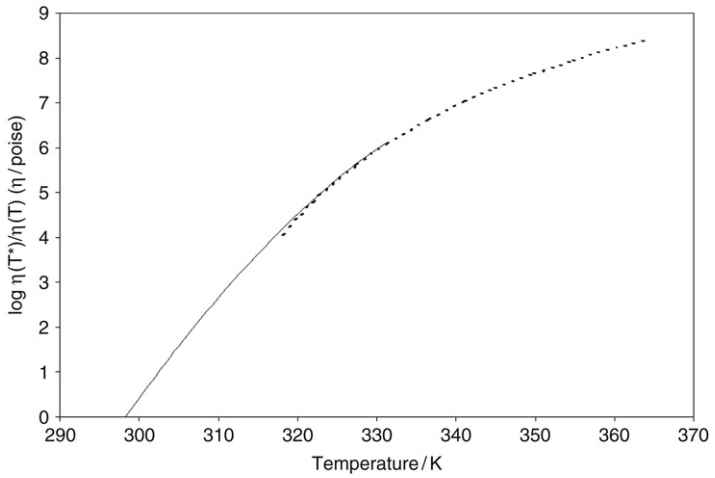

Fig. 1. The viscosity of PDE [27]. The dashed line corresponds to the expression for the viscosity above T_c given by Eq. (9), namely the VFT equation. The full line represents the viscosity obtained using Eq. (8) below T_c.

that fits the data of different fragile supercooled glass forming liquids [26,27,62,63], T^* is a reference temperature, taken here as T_g.

We have studied four supercooled fluids, namely, phenyl salicylate (salol), phenolphthaleine-dimethyl-ether (PDE), orthoterphenyl (OTP) and tri-naphthylbenzene (TNB). Fitting the data for their viscosity in the region below T_c using Eq. (8), in Table 1, we present the values for the parameters of the equation for these liquids. On the other hand, for temperatures above T_c, the experimental data fit indeed a VFT equation, that is,

$$\log \frac{\eta(T^*)}{\eta(T)} = A - \frac{B}{T - T_0}. \tag{9}$$

The values of the parameters of Eq. (9) for the same liquids are given in Table 2. In both Tables 1 and 2 we present the values of the χ^2 test and the correlation coefficient R^2 for each fit. The χ^2 test is a statistical test that measures the differences between experimental an theoretical distributions. The correlation coefficient R^2 indicates de degree of linear dependence between the experimental and fit values and must be a number close to 1 to have a good fit. As an example, in Figs. 1 and 2 we present the plot of both Eqs. (8) and (9) for the viscosity of OTP and PDE in the regions below and above respectively. The derivative analysis presented by Sickel et al. [26,27] permits us to carry on three calculations that give a physical support to our proposal, namely, Eq. (8) to fit the values of the viscosity below T_c.

We shall present four physical features that support our Eq. (8) throughout this work.

Firstly, as we have discussed in a previous work [56], it is easily seen that in the vicinity of T_c both description, Eqs. (8) and (9) overlap as one may observe in Figs. 1 and 2. A similar behavior may be observed in the case of salol and TNB. Since the description in terms of the derivative analysis has been useful to distinguish differences between the two dynamic regimes in a supercooled liquid, we find the temperature T_c' where both descriptions intersect, using the fact that,

$$\Theta_{T<T_c}(T_c') = \Theta_{T>T_c}(T_c') \tag{10}$$

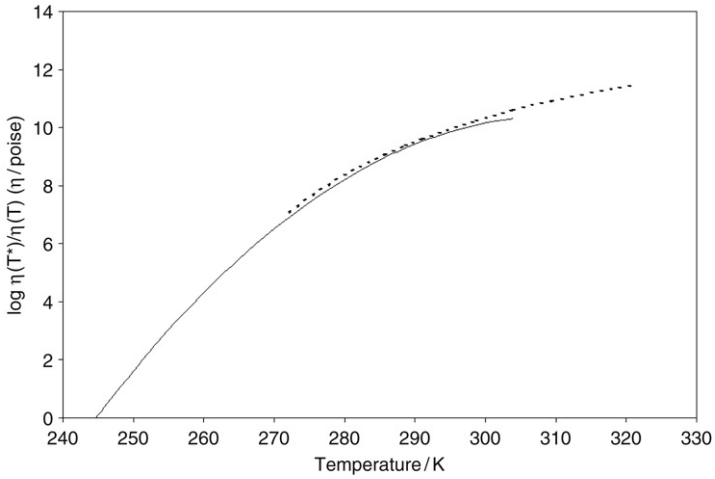

Fig. 2. The viscosity of OTP [6127]. The dashed line corresponds to the expression for the viscosity above T_c given by Eq. (9), namely the VFT equation. The full line represents the viscosity obtained using Eq. (8) below T_c.

Table 3
Values of the temperatures T_g and T_c and the value for T_c' predicted from the intersection given by Eq. (10)

Glassformer	T_g (K)	T_c (K)	T_c' (K)
Salol	220	265	260
PDE	294	325	327
OTP	240	290	283
TNB	342	410	412

where Θ is given by Eq. (7). In Table 3 we present the values for T_c' and the reported values for T_c, and we find that they both present a very good agreement,may be taken, within a very small deviation, as equal.

Eq. (10) allows us to give a second physical interpretation to Eq. (8). If we evaluate Θ for Eq. (8), we find that

$$\Theta = T - T_A \tag{11}$$

and for the VFT equation (9),

$$\Theta_{VFT} = -\frac{T - T_0}{2}. \tag{12}$$

Since both expressions (11) and (12) intersect at T_c, Eq. (10) we may find an expression for the empirical temperature T_A in Eq. (8) in terms of the temperatures T_A in Eq. (8) in terms of the temperatures T_c and T_0 that have a well known physical meaning, that is,

$$T_A = \frac{3T_c - T_0}{2} \tag{13}$$

thus, the temperature is not an independent parameter. In Fig. 3, we may observe the good linear fit between the values of T_A', the value of T_A evaluated by Eq. (13), and the value T_A that appears in Eq. (8).

The third physical fact that we may analyze using Stickel's method is the assertion by several authors, as we have already mentioned, that two different VFT equations may be fitted for each one of the two regimes regions. If we now propose a VFT equation for $T > T_c$,

$$\left[\log \frac{\eta(T^*)}{\eta(T)}\right]_{T>T_c} = A_1 - \frac{B_1}{T - T_{01}} \tag{14}$$

and a second VFT equation for $T < T_c$,

$$\left[\log \frac{\eta(T^*)}{\eta(T)}\right]_{T<T_c} = A_2 - \frac{B_2}{T - T_{02}} \tag{15}$$

using the fact that Θ must intersect at T_c, Eq. (10), we obtain

$$T_{01} = T_{02} \tag{16}$$

that contradicts the fact that two different VFT equations may be fitted in the regions above and below for temperatures T_c.

Thus, following the three results obtained via Stickel's method, Eq. (8) is a good proposal to fit the viscosity data below T_c.

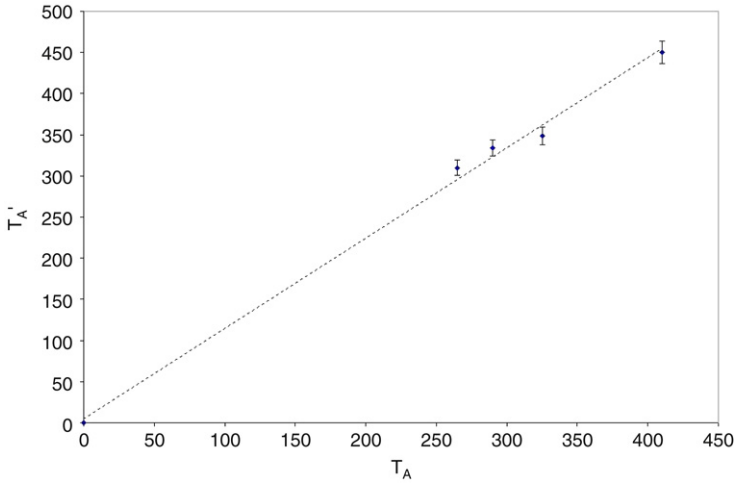

Fig. 3. Temperature T_A given in Eq. (8) as a function of the temperature T'_A evaluated by Eq. (13). The error bars are of a 3%. Thus both values are in a very good agreement.

Table 4
Values for the radii and glass transition temperatures of different hosts [35,45]

Host	r_H (nm)	T_g (K)
PDBE	0.47	346
FDE	0.45	318
ODE	0.43	285
Salol	0.35	218
CDE	0.43	310
mTCP	0.42	205
TNB	0.46	342
OTP	0.38	243
PDE	0.41	294

Table 5
Values for the radii of the tracers [35,47]

Tracer	r_T (nm)
TTI	0.38
Rubrene	0.8
Tetracene	0.5
ONS-A	0.72
ACR	0.38

3. The diffusion coefficient

As far as the diffusion process is concerned, the crossover that occurs at T_c between the SE regime and its breakdown from $\xi = 1$ to $\xi < 1$ is due to the inhomogeneity of the system as it is brought towards T_g. While supercooling, the viscosity of the liquid increases faster than the decrease in the diffusion coefficient. This decoupling depends largely on the relative size of the tracer with respect to the size of the liquid molecules and on the temperature region where the liquid is studied. In Tables 4 and 5, we present van der Waals radii for different hosts and tracers.

In order to quantify the breakdown of the SE relation below T_c we have analyzed the dependence of the diffusion coefficient with the viscosity for three liquids, using in each case three tracers of different sizes. In Figs. 4–6, we have plotted $\log \eta(T^*)/\eta(T)$ vs. $\log D(T)/D(T^*)$ for TNB, OTP and PDE, respectively, using for the viscosity the form given by Eq. (8) for $T < T_c$, and experimental data for the diffusion coefficients [39,41,47], providing the exponent ξ as the slope of each straight line. We have not made this analysis in the case of salol, since only one tracer, namely, TTI, has been reported in the literature [41]. The value of ξ in salol has been already reported in Ref. [56]. In the case of TNB, Fig. 4, we can see that the smaller value of ξ corresponds to the smallest tracer, TTI, while the larger value corresponds to the larger tracer, rubrene. This same behavior is observed in the case of OTP, Fig. 5 and PDE, Fig. 6. The different values of ξ obtained in our work are given in Table 6.

We may compare the experimental values for the diffusion coefficient with those obtained from the Stokes–Einstein equation, Eq. (2) and the modified fractional expression, Eq. (3). For example, in Fig. 7, we present the experimental values for the diffusion coefficient of TTI in TNB, and compare them with those that may be obtained from the SE relation, Eq. (2),

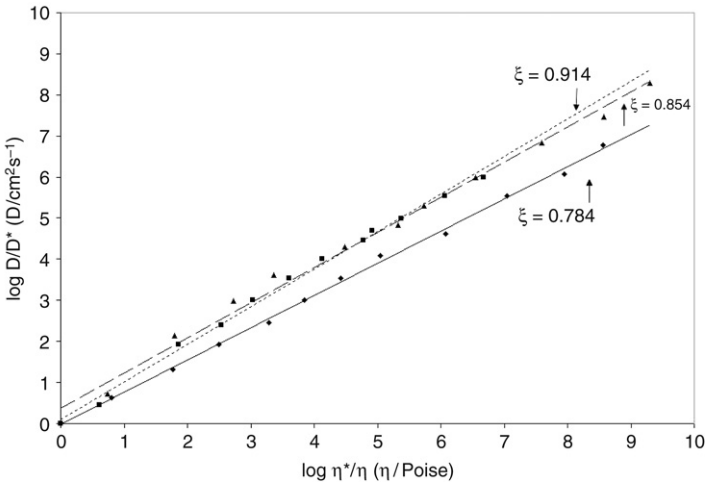

Fig. 4. Diffusion coefficients for tracers in TNB in terms of the viscosity. Experimental values for TTI (♦), rubrene (■) and tetracene (▲) [47]. The full, dotted and dashed lines represent the linear fits for TTI, rubrene and tetracene, respectively, where ξ is the slope in each case.

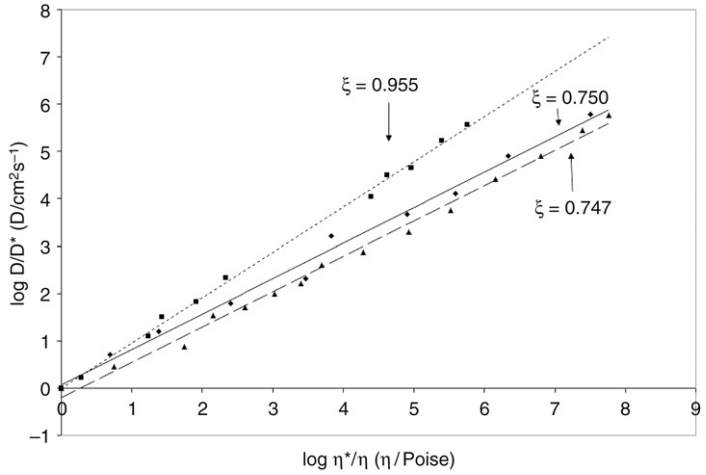

Fig. 5. Diffusion coefficients for tracers in OTP in terms of the viscosity. Experimental values for TTI (♦), rubrene (■) and tetracene (▲) [39]. The full, dotted and dashed lines represent the linear fits for TTI, rubrene and tetracene, respectively, where ξ is the slope in each case.

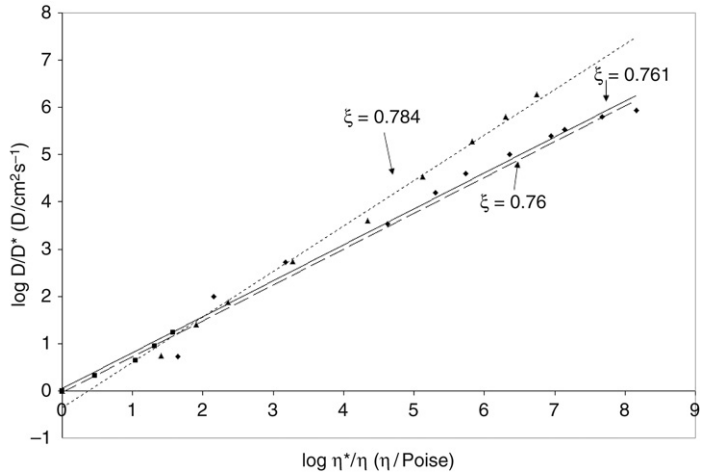

Fig. 6. Diffusion coefficients of tracers in PDE in terms of the viscosity. Experimental values for TTI (♦), ONS-A (▲) and ACR (■) [41]. The full, dashed and dotted lines represent the linear fits for TTI, ONS-A and ACR, respectively, where ξ is the slope in each case.

Table 6
Values for the exponent ξ for different tracers in TNB, OTP and PDE obtained in this work and the corresponding correlation coefficient R^2 for the linear fit

ξ	TTI	R^2	Tetracene	R^2	Rubrene	R^2	ONS-A	R^2	ACR	R^2
TNB	0.784	0.998	0.854	0.992	0.914	0.995				
OTP	0.75	0.991	0.747	0.994	0.955	0.997				
PDE	0.761	0.984					0.962	0.998	0.76	0.977

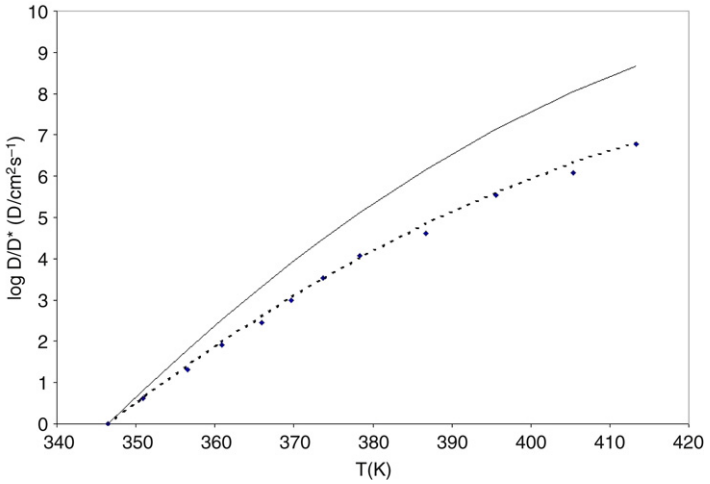

Fig. 7. TTI in TNB. Comparison among the experimental data for the diffusion coefficient (♦) [47], the values obtained by the SE Eq. (2), (full line) and the values obtained by the modified expression in terms of ξ, Eq. (3) (dotted line) in terms of the temperature.

and the modified expression, Eq. (3). It is easily seen that the experimental data fit quite well with the relation that results from the breakdown of the SE regime for temperatures below T_c. This same result may be obtained with the other tracers in TNB and as well as for PDE and OTP and their corresponding tracers.

The fourth physical feature that supports our equation for the viscosity below T_c is that we obtain a similar result as the one obtained by Heuberger and Sillescu [35]. They suggest that a temperature shift ΔT in the temperature dependence of the diffusion coefficient evaluated via the SE equation, Eq. (2), has the same effect as evaluating this coefficient through the breakdown SE expression, Eq. (3). They evaluate both expressions using the VFT equation, and equating both results they find the value of the temperature shift ΔT in terms of the exponent ξ. We repeat this calculation using our expression for the viscosity below T_c, Eq. (8), instead of the VFT equation and obtain the ΔT that makes both calculations coincide.

Using the SE equation, Eq. (2), we may write for the diffusion coefficient

$$\log \frac{T_g D_\eta (T)}{T D_0} = C (T_A - T)^2 + E. \tag{17}$$

Now, introducing a temperature shift ΔT,

$$\log \frac{T_g D_\eta (T + \Delta T)}{(T + \Delta T) D_0} = C (T_A - T - \Delta T)^2 + E. \tag{18}$$

The power law assumption changes C into ξC,

$$\log \frac{T_g D_\xi (T)}{T D_0} = \xi C (T_A - T)^2 + E. \tag{19}$$

Equating the lhs of Eqs. (18) and (19) one finds

$$\xi - 1 = -2 \frac{\Delta T}{T_A - T}$$

or alternatively,

$$\Delta T = \frac{1}{2} (1 - \xi) (T_A - T) . \tag{20}$$

As an example, in Fig. 8, we present the behavior of the diffusion coefficient of TTI in TNB. It is easily seen that the diffusion coefficient, given by the SE equation, shifted in temperature by the shift given in Eq. (20) fits well with the experimental data for the same coefficient. We find the same behavior for the other tracers in TNB, and for the case of PDE and OTP and

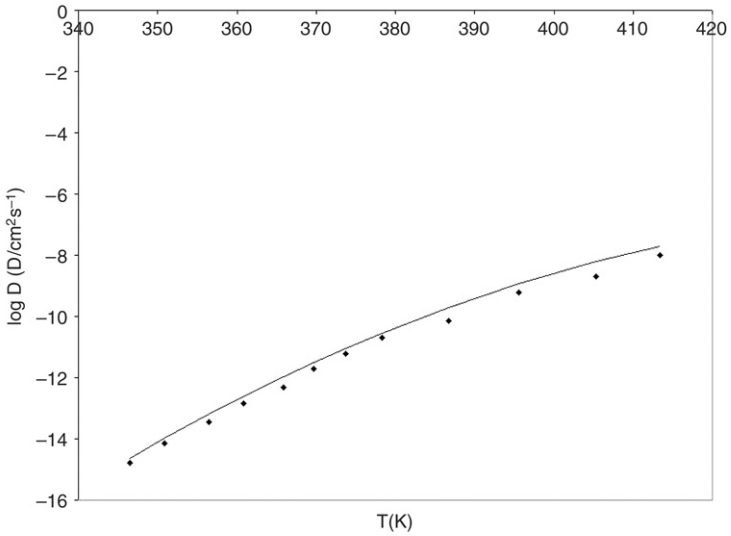

Fig. 8. TTI in TNB. Comparison between the experimental data for the diffusion coefficient (♦) [47] and the values obtained by means of the temperature shift given in Eqs. (18) and (20) in terms of the temperature (full line).

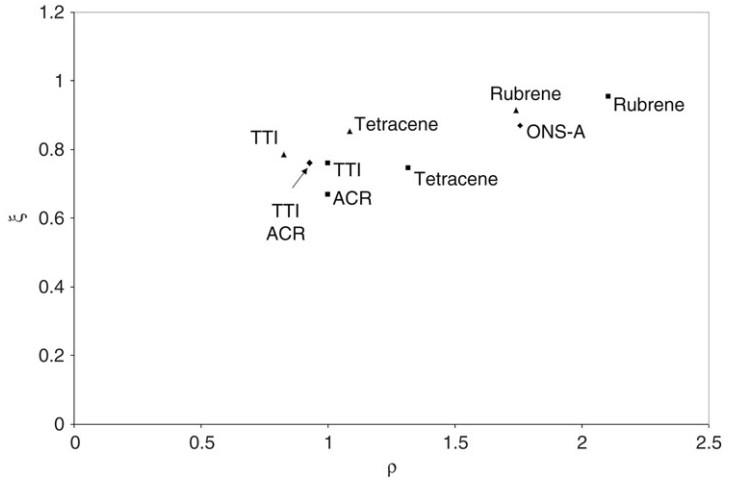

Fig. 9. The exponent ξ, obtained in this work, in terms of the ratio of the radii, $\rho = \frac{r_T}{r_H}$ [35] for different tracers in different hosts, PDE (♦), OTP (■) and TNB (▲).

their corresponding tracers. In each case, the temperature shift ΔT depends on the corresponding tracer in a host and the value for T_A that appears in Eq. (8). Thus, an horizontal shift on the diffusion coefficient may have the same influence of the breakdown of the SE relation through the exponent ξ.

Furthermore, we have studied the dependence of ξ with the ratio ρ between the radius of the host and that of the tracer, that is,

$$\rho = \frac{r_T}{r_H}$$

where r_T and r_H are the radii of the tracer and the host,respectively, given in Tables 4 and 5. In Fig. 9, we have plotted values of ξ for different tracers vs the ratio ρ for TNB, OTP and PDE. We can observe that the dependence of ξ on the ratio of the radii is clearly an increasing function. In Fig. 10, we present values of ξ for the tracer TTI in nine different host liquids. Fig. 10 may indicate that the exponent ξ may depend on other parameters. For example, in Fig. 11 we present the dependence of ξ on the glass transition temperature T_g of the host.

Analyzing our results, we find important evidence of the enhancement of the diffusion processes in small tracers. This behavior decreases as the size of the tracer increases. This suggests that the Stokes–Einstein equation works well for tracers large enough when compared with the size of the host molecule.

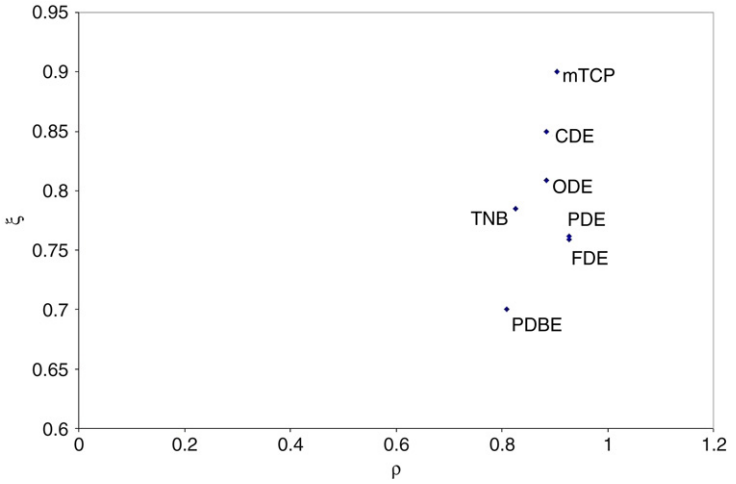

Fig. 10. The exponent ξ, evaluated in this work and those given in reference [35] in terms of the ratio of the radii $\rho = \frac{r_T}{r_H}$ for TTI in different hosts.

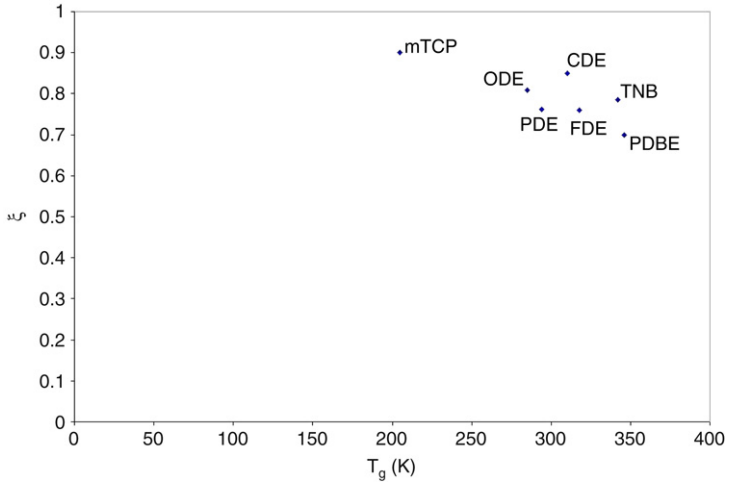

Fig. 11. The exponent ξ, evaluated in this work and those given in reference [35], in terms of the glass transition temperatures for TTI in different hosts.

4. Conclusions

As it has been discussed, for more than a decade, important experimental results have shown that the VFT equation for the viscosity is not valid to fit the experimental data for the viscosity in the whole range of temperatures from T_g to T_m. We present an expression for the viscosity in the region below T_c region that depends on a temperature T_A that may be expressed in terms of the isoentropic temperature T_0 and T_c. We also show that two different VFT equations may be used to fit separately the regions below and above T_c.

For small tracers we observe that as the temperature is lowered towards T_g, in the region below the crossover temperature T_c, the SE relation (2) breaks down presenting a pronounced enhancement of the diffusion of the tracer though an exponent $\xi < 1$, whose value depends on the relative size of the tracer with respect to the host liquid and the glass transition temperature of the host. We have noted that introducing a temperature shift on the diffusion coefficient may have the same effect as the one observed in the breakdown of the SE equation. Particularly, the proper supersposition principle $T - t$ may be used to replace the use of the fractional power expression in terms of ξ in the diffusion coefficient in terms of the viscosity.

Several scenarios may be taken into consideration to deal with the explanation of the decoupling between the viscosity and the translational diffusion coefficient. The enhancement of the tracer diffusion coefficient over other kinds of relaxation processes such as those described by the variables given in Eq. (4) may be explained assuming that, through supercooling at low temperatures in the vicinity of T_g, the dynamics of the liquid becomes heterogeneous. One may picture mobile or "fluid-like" regions that are responsible of the translational displacements, and less mobile "frozen solid-like" regions that determine the structural relaxation. The dynamic heterogeneity provokes that the fluctuating processes in the liquid occur

at different scales of length and time. On supercooling liquids, below T_c, besides the conventional hydrodynamic modes, the hopping mode presents an important contribution [48,49,51]. Using these ideas, one may find several models in the literature – such as the obstruction model – where the diffusion of a tracer is modeled in terms of a diffusion process through obstructions [49], and the simulations of the diffusion on three dimensional cubic lattices [50,51], both reproducing the same results on the enhancement of the diffusion for small tracers.

Acknowledgements

The authors wish to acknowledge economical support from DGAPA-UNAM Proyecto IN 119606 and CONACYT-SEP C01-47070. We thank María Teresa Vázquez Mejía, Sara Jiménez Cortes and Raúl Reyes Ortiz.

References

[1] H. Vogel, Z. Phys. 22 (1921) 645.
[2] G.S. Fulcher, J. Am. Ceram. Soc. 8 (1925) 339.
[3] G. Tamann, G. Hesse, Z. Anorg. Allg. Chem. 156 (1926) 245.
[4] J. Gerardin, S. Mohanti, U. Mohanti, J. Chem. Phys. 119 (2003) 4473.
[5] E. Donth, The Glass Transition, Relaxation Dynamics in Liquids and Disordered Materials, Springer Verlag, Berlin Heidelberg, 2001.
[6] M. Beiner, J. Korus, E. Donth, Macromolecules 30 (1997) 8420.
[7] M. Beiner, S. Kahle, E. Hempel, K. Schöter, E. Donth, Macromolecules 31 (1998) 8973.
[8] M. Beiner, S. Kahle, E. Hempel, K. Schröter, E. Donth, Europhysics Lett. 44 (1998) 321.
[9] S. Kahle, E. Hempel, M. Beiner, R. Unger, K. Schöter, E. Donth, J. Mol. Struct. 749 (1999) 149.
[10] D. Gómez, A. Alegría, A. Arbe, J. Colmenero, Macromolecules 34 (2001) 503.
[11] K.L. Ngai, Phys. Rev. E 57 (1998) 7346.
[12] C. León, K.L. Ngai, J. Chem. Phys. 110 (1999) 11585.
[13] C. León, K. Ngai, J. Phys. Chem. B 103 (1999) 4045.
[14] L. Andreozzi, M. Faetti, M. Giordano, D. Leporini, J. Phys.: Condensed Matter 11 (1999) A131.
[15] C.A. Angell, J. Non-Cryst. Solids 131–133 (1991) 13.
[16] F.H. Stillinger, Science 267 (1995) 1935.
[17] B. Frick, D. Richter, Science 267 (1995) 1939.
[18] R. Böhmer, K.L. Ngai, C.A. Angell, D.J. Plazek, J. Chem. Phys. 99 (1993) 4201.
[19] J. Colmenero, A. Alegría, J.M. Alberdi, F. Álvarez, B. Frick, Phys. Rev. B 44 (1991) 7321.
[20] M.D. Ediger, C.A. Angell, S.R. Nagel, J. Phys. Chem. 100 (1996) 13200.
[21] C.A. Angell, P.H. Poole, J. Shao, Il Nuovo Cimento 16D (1994) 993.
[22] B. Frick, D. Richter, Phys. Rev B 47 (1993) 14795.
[23] E. Rössler, U. Warschewski, P. Eiermann, A.P. Sokolov, D. Quitmann, J. Non-Cryst. Solids 172–174 (1994) 113.
[24] A. Sokolov, A. Kisliuk, D. Quitmann, A. Kudlik, E. Rössler, J. Non-Cryst. Solids 172–174 (1994) 133.
[25] A. Sokolov, E. Rössler, A. Kisliuk, D. Quitmann, Phys. Rev. Lett. 71 (1993) 262.
[26] F. Stickel, E.W. Fischer, R. Richert, J. Chem. Phys. 102 (1995) 6251.
[27] F. Stickel, E.W. Fischer, R. Richert, J. Chem. Phys. 104 (1996) 2043.
[28] C. Hansen, F. Stickel, T. Berger, R. Richert, E.W. Fischer, J. Chem. Phys. 107 (1997) 1086.
[29] C. Hansen, F. Stickel, R. Richert, E.W. Fischer, J. Chem. Phys. 108 (1998) 6408.
[30] R. Richert, C.A. Angell, J. Chem. Phys. 108 (1998) 9016.
[31] K. Duvvuri, R. Richert, J. Chem. Phys. 117 (2002) 4414.
[32] R. Richert, K. Duvvuri, L.T. Duong, J. Chem. Phys. 118 (2003) 1828.
[33] L.M. Wang, R. Richert, J. Chem. Phys. 121 (2004) 11170.
[34] E. Rössler, Phys. Rev. Lett. 65 (1990) 1595.
[35] G. Heuberger, H. Sillescu, J. Phys. Chem. 100 (1996) 15255.
[36] C.H. Wang, S.S. Gong, J. Chem. Phys. 117 (2002) 4896.
[37] M.T. Cicerone, F.R. Blackburn, M.D. Ediger, Macromolecules 28 (1995) 8224.
[38] M.T. Cicerone, F.R. Blackburn, M.D. Ediger, J. Chem. Phys. 102 (1995) 471.
[39] M.T. Cicerone, M.D. Ediger, J. Chem. Phys. 104 (1996) 7210.
[40] D.B. Hall, D.D. Deppe, K.H. Hamilton, A. Dhinojwala, J.M. Torkelson, J. Non-Cryst. Solids 235-237 (1998) 48.
[41] I. Chang, F. Fujara, B. Geil, G. Heuberger, T. Mangel, H. Sillescu, J. Non-Cryst. Solids 172–174 (1994) 248.
[42] D. Ehlich, H. Sillescu, Macromolecules 23 (1990) 1600.
[43] M.T. Cicerone, M.D. Ediger, J. Phys. Chem. 97 (1993) 10489.
[44] F. Fujara, B. Geil, H. Sillescu, G. Fleischer, Z. Phys. B Condensed Matter 88 (1992) 195.
[45] I. Chang, H. Sillescu, J. Phys. Chem. B 101 (1997) 8794.
[46] A. Veniamov, H. Sillescu, Macromolecules 32 (1999) 1828.
[47] F.R. Blackburn, C.Y. Wang, M.D. Ediger, J. Phys. Chem. 100 (1996) 18249.
[48] S. Battacharyya, B. Bagchi, J. Chem. Phys. 107 (1997) 5852.
[49] J.F. Douglas, D. Leporini, J. Non-Cryst. Solids 235–237 (1998) 137.
[50] M.T. Cicerone, P.A. Wagner, M.D. Ediger, J. Phys. Chem. B 101 (1997) 8727.
[51] C.Y. Wang, M.D. Ediger, J. Chem. Phys. B 104 (2000) 1724.
[52] X. Xia, P.G. Wolynes, J. Phys. Chem. B 105 (2001) 6570.
[53] F.H. Stillinger, P.G. Debenedetti, J. Phys. Chem. B 109 (2005) 6604.
[54] K.L. Ngai, J. Phys. Chem. B 103 (1999) 10684.
[55] K.L. Ngai, J.H. Magill, D.J. Plazek, J. Chem. Phys. 112 (2000) 1887.
[56] P. Goldstein, L.S. García-Colín, L.F. del Castillo, Physica A 275 (2000) 325.
[57] D. Kivelson, G. Tarjus, X. Zhao, S.A. Kivelson, Phys. Rev. E 53 (1996) 751.
[58] E. Rössler, J. Chem. Phys. 92 (1990) 3725.
[59] K. Schröter, E. Donth, J. Chem. Phys. 113 (2000) 9101.
[60] S. Kahle, K. Schröter, E. Hempel, E. Donth, J. Chem. Phys. 111 (1999) 6462.
[61] M.L. Williams, R.F. Landel, J.D. Ferrry, J. Am. Chem. Soc. 77 (1955) 3701.
[62] D.J. Plazek, C.A. Bero, I.C. Chay, J. Non-Cryst. Solids 172–174 (1994) 181.
[63] D.J. Plazek, J.H. Magill, J. Chem. Phys. 45 (1966) 3038.